



# Experimental and modeling study of the fate and behavior of thiobencarb in clay and sandy clay loam soils

A. F. El-Aswad<sup>1</sup> · M. R. Fouad<sup>1</sup> · M. I. Aly<sup>1</sup>

Received: 28 April 2022 / Revised: 13 June 2023 / Accepted: 16 October 2023 / Published online: 15 November 2023  
© The Author(s) 2023

## Abstract

Pesticides cannot be stopped today, but at the same time, it is impossible to accept the use of them without understanding their fate and behavior in the environment to accomplish their purpose and avoid their risks. To determine the behavior of thiobencarb in two common Egyptian soil types, clay soil and sandy clay loam soil, the adsorption–desorption isotherms, leaching, and dissipation processes were tested. Also, the obtained experimental data were modeled to predict the different processes and to determine the characteristic parameters of each process. Thiobencarb residues were measured by GC–MS and UV–Vis Spectrophotometer. The results indicated that thiobencarb dissipation is consistent with the 1st-order kinetic model, and the half-life is 10.61 days in clay soil and 10.24 days in sandy clay loam soil. The pseudo-second-order kinetic model and Freundlich isotherm model fit the experimental adsorption and desorption data. Both thiobencarb adsorption and mobility were significantly correlated. Compared with sandy clay loam soil, thiobencarb adsorption was greater in clay soil, producing *S*-type isotherms, whereas desorption in clay soil was lower, producing *C*-type isotherms. The leaching of thiobencarb is moderate in clay soil and sandy clay loam soil. However, it was significantly more leachable in sandy clay loam soil than in clay soil. Hence, it is very important to manage and pay attention to the irrigation of rice crop in order to prevent the leaching potential of herbicide thiobencarb and the threat to groundwater resources, as well as to avoid reducing weed control efficiency.

**Keywords** Thiobencarb · Adsorption · Dissipation · Leaching · Kinetic models · Isotherm models

## Introduction

There is no expectation that pesticides will be dispensed in the foreseeable future. Pesticides play an essential role in pest control, since they improve the quality, quantity, and sustainability of agricultural products. Approximately two million tons of pesticides are applied each year (Bondarova and Fedorova 2021; Lykogianni et al. 2021). More than 99% of applied pesticides are spread in the environment, damaging soil, water, and other organisms (Ge et al. 2017). It is possible for the soil to be contaminated with pesticides by direct use as well as indirect contact such as agriculture

spray drift, run-off, aerial sprayers, sub-surface drainage and leaching. Consequently, pesticides can penetrate into deep layers of the soil, increasing the risk of groundwater contamination (Bhushan and Pathma 2021; Mojiri et al. 2020; Yang et al. 2021).

In soil, the fate and behavior of pesticides are determined by different processes, including adsorption, leaching, volatilization, and degradation (Sondhia 2019). These processes are influenced by a variety of factors, including characteristics of the soil (soil texture, organic matter (OM) content), the physicochemical properties of pesticides (solubility in water, sorption coefficient), environmental conditions (temperature, humidity), and practices (rate and method of application) (Das et al. 2015; Tudi et al. 2021). Additionally, persistence, movement, and bioactivity of herbicides are affected by their adsorption–desorption processes (Palma et al. 2015; Sarkar et al. 2020).

The equilibrium state of either adsorption process or desorption process was usually achieved within a few hours to a day, but sometimes it required a few days or even months

---

Editorial responsibility: Maryam Shabani.

✉ A. F. El-Aswad  
ahmed.elasouad@alexu.edu.eg

<sup>1</sup> Pesticide Chemistry and Technology Dept., Faculty of Agriculture, Alexandria University, 21545-El-Shatby, Alexandria, Egypt



(Shankar et al. 2020). Adsorption kinetics, which are used to determine the rate of adsorption, are always described by empirical approaches that are based on different kinetic models (Rodrigues and Silva 2016). The Elovich equation is widely used in chemisorption kinetics and is suitable for heterogeneous surfaces. It assumes that the adsorption rate decays exponentially as the amount adsorbed increases (Senthilkumar et al. 2010). The model of intraparticle diffusion is used to explain the adsorption process through porous adsorbents (Itodo et al. 2010). The pseudo-first-order and pseudo-second-order models are both commonly used for describing soil sorption kinetics (Pan and Xing 2010). In addition, about 15 adsorption isotherm models have been developed and used (Foo and Hameed 2010). The most popular adsorption isotherm models could have two, three, four, or five parameters. There are numerous experimental adsorption data that have been characterized accurately using Freundlich isotherm model, which can be applied to both monolayer and multilayer adsorption (Yang 1998). The Langmuir isotherm model originally was used to describe gas adsorption on the solid surfaces, then it has been modified so that it fits solute adsorption on solid surfaces in solutions (Rajahmundry et al. 2021). A three-parameter adsorption isotherm model (Redlich–Peterson) avoids the inaccuracies of Freundlich and Langmuir models (Chen et al. 2022). In general, modeling the behavior of pesticide in soil reduces the cost and time, and it also predicts its behavior under various conditions.

Upon reaching the soil, pesticides are lost via two processes, transport and degradation. The degradation rate of pesticides is dependent on pesticide properties, soil characteristics, and environmental conditions (Rahman et al. 2020). Pesticides leaching in soil and contaminating the groundwater are extremely harmful to the environment (El-Aswad et al. 2002). The leaching of herbicides may also play a role in reducing their activity (Peek and Appleby 1989). The mobility potential of different pesticides in soils could be classified depending on the physicochemical properties of pesticides as well as short-term leaching tests (Gustafson 1989). Several researchers evaluated the leaching potential of pesticides to determine which compounds deserve longer consideration and may require more expensive studies of leaching (Spadotto 2002).

Thiobencarb (carbamate group) is a herbicide widely used to control weeds in rice fields in many countries, including Egypt. However, there is a paucity of literature describing its environmental behavior. Accordingly, this study aimed to determine the extent of the potential contamination of the environment, especially the groundwater, with thiobencarb. By studying adsorption–desorption kinetics and isotherms, soil mobility, and dissipation under laboratory conditions, the behavior of this compound was determined in two Egyptian soil types and modeled under various conditions.

## Materials and methods

### Chemicals

Technical grade 97.0% a.i. of thiobencarb (S-4-chlorobenzyl diethyl thiocarbamate) was obtained from Shandong San Young Industry Co., Ltd. Calcium chloride (CaCl<sub>2</sub>), potassium iodide (KI), anhydrous sodium sulfate (Na<sub>2</sub>SO<sub>4</sub>), magnesium sulfate (MgSO<sub>4</sub>), sodium thiosulphate (Na<sub>2</sub>S<sub>2</sub>O<sub>3</sub>), silver nitrate (AgNO<sub>3</sub>), hydrochloric acid (HCl), sulfuric acid (H<sub>2</sub>SO<sub>4</sub>), hydrogen peroxide (H<sub>2</sub>O<sub>2</sub>), and starch indicator, also commercial solvents including methanol, ethanol, acetone and acetonitrile were purchased from Algomhoria Chemical Co., Alexandria, Egypt. Solvents HPLC-grade methanol, dichloromethane, *n*-hexane and acetonitrile were purchased from Sigma-Aldrich Co. (Spruce Street, Louis., MO, USA).

### Tested soils

Experiments were performed on two common Egyptian soil types, clay and sandy clay loam. The samples were taken from the soil surface layer (0–20 cm) of different locations that had no history of pesticide use. Samples of alluvial soil were taken from the Agricultural Research Station, Abis farm, Faculty of Agriculture, University of Alexandria and the samples of calcareous soil were taken from the Elnahda region, Elamria, Alexandria Governorate. Physical and chemical properties of the soil were determined by the Department of Soil and Water Sciences, Faculty of Agriculture, University of Alexandria, and are given in Table 1. The soil was air-dried, ground, and sieved using a 2-mm sieve before being used. The texture of the soil was determined using the hydrometer method (Holliday 1990). The OM content was determined by dichromate oxidation according to the Walkley–Black method (Nelson and Sommers 1996).

**Table 1** Physical and chemical properties of tested soils

Properties		Soil I	Soil II
Particle Size distribution (%)	Clay	42	20
	Silt	18	13
	Sand	40	67
Texture class		Clay	Sandy clay loam
Water holding capacity (mL)		46	38
EC (m mhos/cm) at 25 °C		1.32	5.03
Soil pH		8.25	8.15
Organic matter content (%)		3.31	1.54
Total carbonate (%)		7.87	44.64



## Determination of thiobencarb

### Spectrophotometric determination and quantification limits

Thiobencarb residues in aqueous samples of sorption and leaching experiments were quantitatively analyzed using UV–VIS Spectrophotometer (Thermo Corporation, evolution 100, Nicolet, Germany). To determine the appropriate wavelength ( $\lambda_{\max}$ ) for thiobencarb with minimum interference, a scanning range of 200–400 nm was used to create a spectral-density curve (*S-D* curve) for pesticide solution containing 5  $\mu\text{g/mL}$ . In order to generate the calibration curve (*C-D* curve), triplicate samples ( $n=3$ ) of known pesticide concentrations (1–50  $\mu\text{g/mL}$ ) were plotted against their respective absorbance levels at the  $\lambda_{\max}$  obtained (Fig. 1). As part of the quality assurance and control process, triplicate samples with a control and blank were used. For each batch, pesticide standards were measured for inter- and intra-batch variation (Abdo et al. 2010).

The limit of blank (LOB), the limit of detection (LOD) and the limit of quantitation (LOQ) refer to the lowest concentration of a pesticide at which measurement is reliable under experimental conditions. To validate the spectrophotometer method, guidelines were calculated for LOB, LOD, and LOQ (El-Aswad et al. 2019). It was obtained that the value of LOB was 0.117  $\mu\text{g/mL}$ , LOD was 0.118  $\mu\text{g/mL}$  and LOQ was 0.196  $\mu\text{g/mL}$ . In addition, the linearity of calibration curve was obtained. The value of LOL (limit of linearity) was determined for the greatest concentration (50  $\mu\text{g/mL}$ ) of the linear shape segment of thiobencarb standard curve. The absorbance of samples above LOL was adjusted to fall within the linear range between LOQ and LOL by dilution and correction.

### GC–MS determination and recovery

Stock solution of thiobencarb was prepared using HPLC-grade methanol (1000 mg/L), by accurately weighing

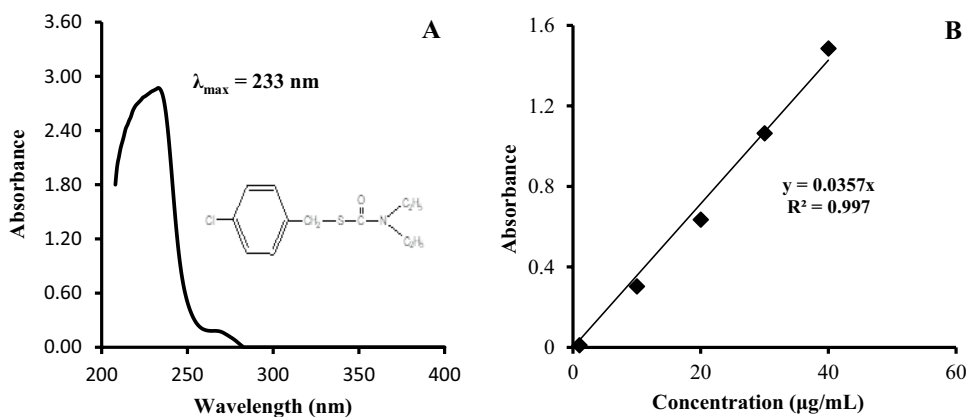
analytical standard into volumetric flask, dissolving and diluting with methanol, and storing at 4 °C in the dark. A fresh working standard solution of thiobencarb was prepared by diluting multiple stock solutions with dichloromethane HPLC-grade. Immediately prior to the samples, an initial standard solution (100  $\mu\text{g/mL}$ ) was measured.

In persistence experiment, the residues of thiobencarb in soil samples were quantitatively determined using GC–MS (Thermo Scientific USA), gas chromatograph Trace 1300 coupled with an EI Mass spectrometer ISQ 7000 model, including TR-50 MS capillary column (30 m in length  $\times$  250  $\mu\text{m}$  in diameter  $\times$  0.25  $\mu\text{m}$  in thickness of film), Spectroscopic detection (high energy electron ionization system (70 eV); MS transfer line temperature 300 °C and ion source temperature 300 °C). The carrier gas (pure helium, 99.995%) with flow rate of 1 mL/min was used. The temperature (60 °C) was initially set, after 2 min, it increased with a rate of 10 °C/min to 100 °C, after 5 min, it increased with a rate of 10 °C/min to 150 °C, after 5 min, it increased with a rate of 10 °C/min to 200 °C, after 5 min, it increased with a rate of 10 °C/min to 250 °C and kept for 20 min. The sample was injected (1  $\mu\text{L}$ ) in a split less mode. Untreated soil samples were homogenized and spiked with standard solutions of thiobencarb (50, 75, and 100  $\mu\text{g/g}$  soil). Two replicates were analyzed at each fortification level. The recovery percentages were 90.89 and 88.34% in clay soil and sandy clay loam soil, respectively (Camara et al. 2020; Redondo et al. 1994).

### Dissipation study of thiobencarb

Thiobencarb dissipation in two soil types; clay and sandy clay loam, was studied under laboratory conditions. A weight of 150 g of each soil type was placed in 500-mL glass bottle and treated with tested pesticide (75  $\mu\text{g a.i./g}$  soil). Three replicates were used for treatments and control. The tested pesticide was dissolved in an amount of distilled water equals 60% of water holding capacity (WHC) of the tested soil. All bottles were incubated at 25 °C up to 84 days.

**Fig. 1** Spectral-Density (*S-D*) curve of thiobencarb **A**. 200 to 400 nm spectra are plotted and clearly show the maximum wavelength is 233 nm and Calibration-Density *C-D* curve of thiobencarb **B** at 233 nm by UV-Spectrophotometric method



A sufficient amount of water was added to replace lost soil moisture during the incubation period (Badawy et al. 2017). The soil was sampled at different times (0, 2, 5, 13, 20, 27, 48, 55 and 84 day). Thiobencarb residue was extracted from air dried soil samples by dichloromethane HPLC-grade. After evaporation of the samples using rotary evaporator, the pesticide residues were dissolved in 1 ml *n*-hexane HPLC-grade and determined using GC–MS (Redondo et al. 1994).

In order to obtain the disappearance curve of thiobencarb in soil, the concentration of pesticide residues against time were plotted. The calculated dissipation rate and half-life value of thiobencarb were assessed by the following equations (Badawy et al. 2017; Yuan et al. 2020).

$$K = \left( \frac{2.303}{t_2 - t_1} \right) \log \left( \frac{C_1}{C_2} \right) \& \quad DT_{50} = \frac{0.6932}{K}$$

where,  $K$  is the dissipation rate,  $C_1$  and  $C_2$  the concentration of pesticide residues at two times  $t_1$  and  $t_2$ , respectively.  $DT_{50}$  is the time required to reduce an amount of a compound by half (Fardillah et al. 2020).

## Adsorption and desorption study of thiobencarb

### Adsorption and desorption kinetics

The batch sorption kinetics experiment was repeated twice on each soil in order to determine the equilibration time for sorption process. Thiobencarb (30  $\mu\text{g}/\text{mL}$ ) in 0.01 M  $\text{CaCl}_2$  solution was used as (1:5 soil: solution). A mechanical shake at 150 rpm has been performed in the dark at room temperature for 1, 2, 3, 6, 12, 24, 30, and 48 h. After centrifuging for 15 min at 4000 rpm, thiobencarb residues in the supernatant were measured with a UV-Visible Spectrophotometer. After adsorption experiments, a decant refill technique was used to carry out the desorption experiments. Fresh 0.01 M  $\text{CaCl}_2$  as

a background solution was used. Based on the final concentration of thiobencarb solution and the weight of the retained solution, the amount of desorbed pesticide was corrected for the amount of solution left behind in the centrifuge sediment (El-Aswad et al. 2019).

The fit kinetic model of the pesticide adsorption–desorption processes was determined using four mathematical kinetic models (Table 2) (Al-Ghouti and Da'ana 2020; Fouad et al. 2019). In tested kinetic models,  $q_t$  = the amount of pesticide adsorbed or desorbed ( $\mu\text{g g}^{-1}$ ) in time  $t$  (h). In Elovich kinetic equation,  $\beta$  = a constant that indicates surface coverage and activation energy required in chemisorption; and  $\alpha$  is a constant related to chemisorption rate ( $\mu\text{g g}^{-1} \text{h}^{-1}$ ). Therefore, a linear relationship should be obtained from a plot of  $q_t$  versus  $\ln t$ , the slope is  $1/\beta$  and the intercept is  $1/\beta \ln(\alpha\beta)$ . In Intraparticle diffusion equation,  $K_d$  = apparent diffusion rate coefficient. A linear relationship should be obtained from a plot of  $q_t$  versus  $t^{1/2}$ , the linear form illustrates that the reaction compatible to parabolic diffusion law (Ahmed et al. 2018). In the equations of Pseudo-first-order rate and Pseudo-second-order rate,  $q_e$  = amount of pesticide adsorbed or desorbed ( $\mu\text{g g}^{-1}$ ) at equilibrium and  $K_1$  = apparent adsorption or desorption rate coefficient,  $K_2$  = rate constant of the second-order adsorption ( $\text{g } \mu\text{g}^{-1} \text{min}^{-1}$ ) (Ezzati 2020). Regarding the boundary conditions  $q = 0$  to  $q = q$  and  $t = 0$  to  $t = t$ , and rearranging, the linearized form can be obtained. If the pseudo-second-order kinetic is applied, the linear relationship should be obtained from the plot of  $t/q$  against  $t$ ,  $K_2$  and  $q_e$  are determined from the intercept and slope of the plot (Carneiro et al. 2015).

### Adsorption and desorption isotherms

Using batch equilibration, the adsorption and desorption isotherms of the pesticide by soil were quantified. Experiments were conducted in duplicate with a soil mass to pesticide

**Table 2** Adsorption and desorption kinetic and isotherm models and their linear forms

Models	Empirical formula	Linear form	Plot
<i>Kinetic models</i>			
Elovich	$\frac{dq_t}{dt} = \alpha \exp(-\beta q_t)$	$q_t = \left(\frac{1}{\beta}\right) \ln(\alpha\beta) + \left(\frac{1}{\beta}\right) \ln t$	$q_t$ vs. $\ln t$
Intraparticle diffusion	$q_t = K_d t^{1/2}$	$q_t = C_{id} + K_{id} t^{1/2}$	$q_t$ vs. $t^{1/2}$
Pseudo-first-order	$q_t = q_e (1 - e^{-k_1 t})$	$\ln(q_e - q_t) = \ln q_e - k_1 t$	$\ln(q_e - q_t)$ vs. $t$
Pseudo-second-order	$\frac{dq_t}{dt} = K_2 (q_e - q_t)^2$	$\frac{1}{q_t} = \frac{1}{q_e} + \left(\frac{1}{k_2 q_e^2}\right) \frac{1}{t}$	$\frac{1}{q_t}$ vs. $\frac{1}{t}$
<i>Isotherm models</i>			
Freundlich	$q_e = K_F C_e^{1/n}$	$\log q_e = \log K_F + \frac{1}{n} \log C_e$	$\log q_e$ vs. $\log C_e$
Langmuir	$q_e = \frac{q_m b C_e}{1 + b C_e}$	$\frac{1}{q_e} = \frac{1}{q_m} + \frac{1}{b q_m C_e}$	$\frac{1}{q_e}$ vs. $\frac{1}{C_e}$
Elovich	$\frac{q_e}{q_m} = K_E C_e \exp\left(-\frac{q_e}{q_m}\right)$	$\ln \frac{q_e}{C_e} = \ln(K_E q_m) - \frac{q_e}{q_m}$	$\ln\left(\frac{q_e}{C_e}\right)$ vs. $q_e$
Redlich-Peterson	$q_e = \frac{K_R C_e}{1 + \alpha_R C_e^\beta}$	$\ln \frac{C_e}{q_e} = \beta \ln C_e - \ln K_R$	$\ln \frac{C_e}{q_e}$ vs. $\ln C_e$



solution ratio of 1:5. Initial thiobencarb concentrations of 10–50  $\mu\text{g mL}^{-1}$  range were prepared in  $\text{CaCl}_2$  solution (0.01 M). After shaking at 150 rpm at room temperature for a time period to achieve equilibrium and centrifugation at 4000 rpm for 15 min, thiobencarb concentration in supernatants was determined by spectrophotometer. The amount of thiobencarb sorbed at equilibrium was calculated,

$$C_s = (C_i - C_e) \times \frac{V}{M_s}$$

where  $C_s$  is the sorbed thiobencarb amount per soil mass unit ( $\mu\text{g g}^{-1}$ ),  $C_i$  is the initial thiobencarb concentration ( $\mu\text{g mL}^{-1}$ ),  $C_e$  is the equilibrium thiobencarb concentration ( $\mu\text{g mL}^{-1}$ ),  $V$  is the solution volume (mL) (Palma et al. 2015) and  $M_s$  is the soil sample weight (g) (El-Aswad et al. 2019; Sun et al. 2011).

The adsorption partition coefficient ( $K_d$ ) is defined as the ratio between the adsorbate concentration in soil and that in solution at equilibrium state,  $C_s = K_d C_e$ . Values of  $K_d$  ( $\text{mL g}^{-1}$ ) can be obtained graphically by plotting  $C_s$  vs.  $C_e$  (Sundaram 1994) or mathematically as a mean corresponded to different concentrations (Cox and Flin 1998). The  $K_d$  value is related to soil organic matter by the following equation,  $K_{om} = (K_d/\%OM) \times 100$ , where  $K_{om}$  is the soil OM partition coefficient; it is related with soil OC by the relation of  $K_{oc} = (K_d/\%OC) \times 100$ , where  $K_{oc}$  is the soil OC partition coefficient; and it is related with soil clay content as  $K_{clay} = (K_d/\%clay) \times 100$ , where  $K_{clay}$  is the clay partition coefficient (Hermosín and Cornejo 1994). Immediately after adsorption experiments, the desorption isotherm experiments were carried out using parallel system.

The experimental adsorption and desorption data were modeled with the Freundlich, Langmuir, Elovich and Redlich-Peterson models (Table 2) (Al-Ghouti and Da'ana 2020; Hamdaoui and Naffrechoux 2007; Ulfa and Iswanti 2020). In the case of Freundlich equation,  $K_f$  is a coefficient indicating the sorption capacity ( $\mu\text{g}^{1-(1/n)} \text{mL}^{-1/n} \text{g}^{-1}$ ) and  $1/n$  is a constant indicating the adsorption affinity. The maximum sorption capacity  $q_m$  ( $\mu\text{g g}^{-1}$ ) could be theoretically determined,  $K_f = q_m/C_o^{1/n}$ , a constant initial concentration  $C_o$  should be used; thus  $\log q_m$  is the obtained value of  $\log q$  for  $C = C_o$  (Ulfa and Iswanti 2020). In Langmuir model,  $q_e$  is the quantity of the adsorbate per weight unit of the adsorbent at equilibrium ( $\mu\text{g g}^{-1}$ ),  $C_e$  the equilibrium concentration of the solution ( $\mu\text{g mL}^{-1}$ ),  $q_m$  the maximum sorption capacity ( $\mu\text{g g}^{-1}$ ) and  $b$  is a constant related to adsorption free energy ( $\text{mL } \mu\text{g}^{-1}$ ) (Martínez-Vitela and Gracia-Fadrique 2020). For the Elovich isotherm equation,  $q_m$  is the Elovich maximum sorption capacity ( $\mu\text{g g}^{-1}$ ) and  $K_E$  is the Elovich equilibrium constant ( $\text{mL } \mu\text{g}^{-1}$ ). The linear relationship should be obtained from the plot of  $\ln q/C_e$  vs.  $q_e$ , the values of  $q_m$  and

$K_E$  are determined from the intercept and slope of the plot (Fouad et al. 2019). On the homogeneous or heterogeneous surfaces, adsorption processes can be modeled by the Redlich-Peterson isotherm model, assuming simultaneous monolayer formation and multi-site adsorption. In which  $\alpha_R$  ( $\mu\text{g}^{-1}$ ) and  $K_R$  ( $\text{mL g}^{-1}$ ) are the Redlich-Peterson constants and  $\beta$  is the Redlich-Peterson exponent. Using the linear form of the plot  $\ln C/q_e$  vs.  $\ln C_e$ , the parameters can be obtained from the slope and the intercept (Matias et al. 2019).

### Validation of the mathematical models

The validity of kinetic and isotherm models was tested using the computation of the determination coefficient ( $R^2$ ) (Varada 2023), the normalized standard deviation ( $\Delta q_e\%$ ) and summed squared error (Manohar et al. 2006) calculated as follows:

$$\Delta q_e(\%) = 100 \times \sqrt{\frac{\sum [(q_e^{\text{exp}} - q_e^{\text{cal}})/q_e^{\text{exp}}]^2}{N - 1}}$$

$$\& \text{SSE} = \sum \frac{(q_{e(\text{exp})} - q_{e(\text{cal})})^2}{q_{e(\text{exp})}}$$

where  $N$  is the number of measurements,  $q_{e(\text{exp})}$  is amount of experimentally pesticide adsorbed,  $q_{e(\text{cal})}$  is amount of calculated pesticide adsorbed.

### Mobility study of thiobencarb

Thiobencarb leaching potential in soil was estimated using bench-scale soil columns in laboratory conditions. In the test, soil was loaded into columns (10 cm in diameter PVC pipes with a 60 cm height and a ceramic plate at the bottom end cap), each column was packed to a known bulk density by using 3 kg of soil (Pérez-Lucas, 2019). Soil column as a control was similarity mixed for consistency. The columns were preconditioned by saturation with 0.01 M  $\text{CaCl}_2$  according to (Tian, 2019). Once established, the flow rate was selected to provide saturated flow conditions and to limit the duration of leaching experiments, thereby decreasing the possibility of pesticide degradation. The solution of KI as water tracer (20 mL 0.5 M) was applied for each column (Fouad 2017). A pesticide solution was applied dropwise to the soil surface of each column, corresponding to 25  $\mu\text{g/g}$  soil. Next, the  $\text{CaCl}_2$  solution was applied, and the leachates (100 mL leachate) were collected. The KI was determined in leachate samples based on the Iodimetric method according to (Vogel et al. 2009). Also, thiobencarb residue was determined in all leachates by UV-Spectrophotometric method.





The leaching potential of pesticide can be predicted by different leaching indicators such as the groundwater ubiquity score ( $GUS_{index}$ ) (Bottoni et al. 1996) and the relative leaching potential ( $RLP_{index}$ ) (Hornsby et al. 1991).  $GUS_{index}$  is calculated using the empirical model proposed by (Gustafson 1989).

$$GUS_{index} = [\log DT_{50}] \times [4 - \log K_{OC}]$$

The  $RLP_{index}$  is basically a ratio of  $K_{OC}$  and  $DT_{50}$ , expressed as follows:

$$RLP = \frac{K_{OC}}{DT_{50}} * 10$$

## Statistical analysis

All experiments were repeated twice. Experimental data were statistically analyzed using Minitab® (16.1.0.0. 2006 Inc) and displayed as mean  $\pm$  standard error (SE).

## Results and discussion

### Dissipation kinetic and the half-life of thiobencarb in soil

The disappearance curve of thiobencarb in the two soil types, clay and sandy clay loam throughout 12 weeks incubation under laboratory conditions is shown in Fig. 2. It was found immediately after treatment that the concentrations of thiobencarb in the two soil types at 0 time were lower than the applied concentration. This might be attributed to the formation of soil-bound residue, which was in the range of 7 to 90% depending on the type of pesticide used and the soil type (Khan and Dupont 1986). Thiobencarb residues were detected in all samples up to 8 weeks of incubation, with concentrations decreasing over time, with the residue

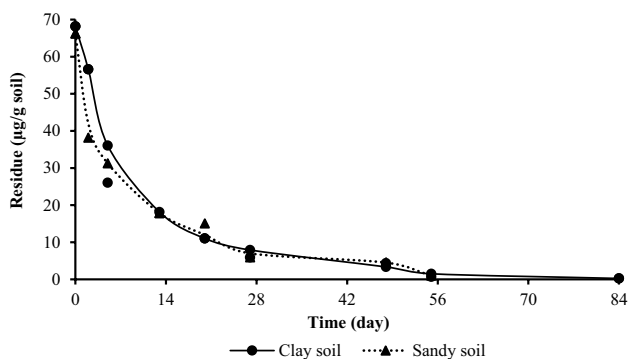


Fig. 2 Disappearance curve of thiobencarb in soils

equivalent to about 1.00% of the initial concentration after 56 days, in two soil types. In addition, thiobencarb residue had been detected in clay soil by the 84th day (0.24  $\mu\text{g/g}$  soil equivalent with 0.36% of the initial concentration). Thiobencarb disappeared from the soil very quickly, just two weeks after treatment, the maximum concentrations were reduced to about one fourth in both soil types of clay and sandy clay loam. Over the next six weeks, there was a slow and gradual decline following this steep decline. There was higher thiobencarb dissipation in the sandy clay loam soil compared to clay soil. It may be due to the fact that clay soil is often richer in organic matter than other soil types (Fouad et al. 2021).

The pesticide residue data in the tested soils should be statistically analyzed to estimate the statistical parameters that describe this process, as suggested by (Likas and Tsiropoulos 2007). Using the formal models in Table 3 one can obtain a linear regression after an appropriate transformation of the pesticide residue. A value of the determination coefficient ( $R^2$ ) for each of the models was calculated in order to select the best fit. In general, ( $R^2 \leq 1$ ), means that the decline curve fits the experimental data better; if  $R^2$  is negative or zero, then the fit will be rejected (Lopez-Lopez et al. 2004). Among all the kinetic models, the first-order model with an  $R^2$  of 0.950 has the highest  $R^2$ , while other models have a  $R^2$  of 0.560 to 0.747 and 0.448 to 0.600 for clay and sandy clay loam soil, respectively. As a consequence, the thiobencarb dissipation in two soils studied fits the 1st-order kinetic model. There have been many studies fitting decline curves to first-order models for a variety of pesticides (Adhya et al. 1987). Thus, the amount of thiobencarb residue was estimated using the first-order kinetics model,  $C_t = C_0 e^{-kt}$ , where  $C_t$  is thiobencarb residue in soil after time  $t$ ,  $C_0$  is the concentration of initial thiobencarb solution, and  $k$  is the constant of first-order rate (Badawy et al. 2017). Thiobencarb dissipated at a rate constant ( $k$ ) of 0.065 in clay soil and 0.068 in sandy clay loam soil, and at an estimated  $DT_{50}$  of 10.61 days in clay soil and 10.24 days in sandy clay loam soil. This is in agreement with previous studies,

Table 3 Determination coefficient ( $R^2$ ) for thiobencarb residues in soil using different dissipation kinetic models

Model	Empirical equation	Soil	$R^2$
Zero order	$C_t = C_0 - kt$	Clay soil	0.560
		Sandy soil	0.600
1st order	$C_t = C_0 e^{-kt}$	Clay soil	0.950
		Sandy soil	0.912
2nd order	$1/C_t = (1/C_0) + kt$	Clay soil	0.747
		Sandy soil	0.564
3rd order	$1/C_t^2 = (1/C_0^2) + 2kt$	Clay soil	0.615
		Sandy soil	0.448

which estimated that thiobencarb has a half-life of 12 days in soil (Redondo et al. 1994). Nevertheless, another study found that thiobencarb had a half-life of 14 to 21 days (Wauchope et al. 1992). The differences in the half-life values can be attributed to the relationship between the persistence of pesticide and the soil characteristics as well as the environmental conditions (Scholz-Starke et al. 2017).

### Adsorption and desorption kinetics of thiobencarb in soil

To study adsorption kinetics, the rate of solute adsorption is measured with respect to time at a constant concentration. Adsorption kinetics describe the adsorption rate and also controls the time of equilibrium (Ahmed et al. 2018). Adsorption–desorption kinetics is therefore essential for understanding the dynamic interactions of various pollutants with solid phases, and it can also be used to predict their fates over time (Et and Shahmohammadi-Kalalagh 2011). Figure 3 shows the adsorption and desorption of thiobencarb in clay and sandy clay loam soil versus time at 30 µg/mL concentration at room temperature. As a consequence of the adsorption and desorption kinetics, there are two distinct stages: the early stage includes a rapid process, then the later stage includes a slow process. There could be a rapid stage due to the filling of surface vacant positions in the soil particles rapidly, then a slow movement, followed by pesticide diffusion into the matrix of soil organic matter and soil minerals (Spuler et al. 2019).

The adsorption rate of thiobencarb onto clay soil and sandy clay loam soil increased during the first six hours of shaking, but then slightly increased at 12 h and reached the

plateau at 48 h of shaking. Therefore, the adsorption–desorption experiments were conducted using 30 h as an equilibrium time. The data displayed graphically in Fig. 3 showed thiobencarb presented a stronger affinity for clay soil than for sandy clay loam soil. This result might be due to clay soil containing more clay and OM than sandy clay soil. The soil clay content is correlated positively with pesticide adsorption (Copaja and Gatica-Jeria 2021).

### Modeling of thiobencarb adsorption and desorption kinetics

In the search for a valid kinetic model that can describe thiobencarb experimental data, there were four different models applied (Elovich, intraparticle diffusion, pseudo-first-order and pseudo-second-order). To determine the kinetic model parameters for thiobencarb, the linearized plot of  $q_e$  (the amount of solute adsorbed) and contact time values are used. The presented results in Table 4, showing that the  $R^2$  value varies from pseudo-second-order (highest value) to pseudo-first-order to Elovich to intraparticle diffusion model (lowest value). Additionally, the results show low values of  $\Delta q_e\%$  and SSE. A model which produces relatively high  $R^2$  and low  $\Delta q_e\%$  and SSE values is known to be the best fit for describing the experimental data (Manohar et al. 2006; Kumar et al. 2018). Also, as seen from Table 4 high values of  $R^2$  ( $> 0.96$ ) and acceptable values of  $\Delta q_e\%$  and SSE for desorption of thiobencarb on clay soil and sandy clay loam soil. Therefore, the pseudo-second-order equation may be more applicable in terms of thiobencarb adsorption and desorption on clay soil and sandy clay loam soil. The Pseudo-second-order

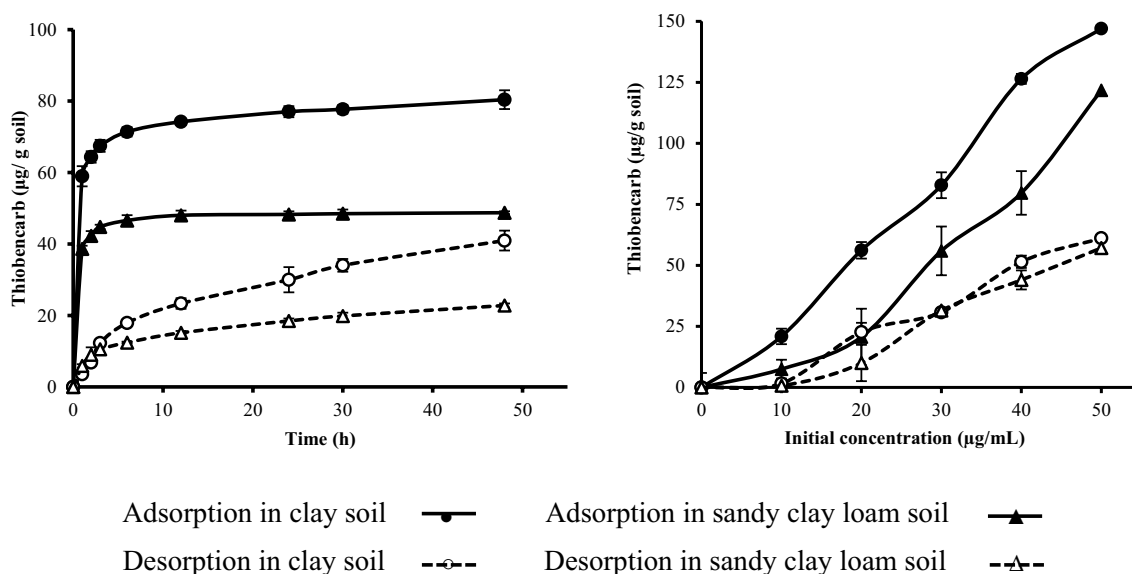


**Fig. 3** Adsorption and desorption kinetics  $\pm$  SE (left) and isotherm  $\pm$  SE (right) of thiobencarb in clay and sandy clay loam soil



**Table 4** Kinetic and isotherm parameters for adsorption and desorption of thiobencarb in clay and sandy clay loam soil

Models	Parameters	Adsorption		Desorption	
		Clay soil	Sandy clay loam soil	Clay soil	Sandy clay loam soil
<i>Kinetic parameters</i>					
Elovich	$\alpha$ ( $\mu\text{g g}^{-1} \text{h}^{-1}$ )	$5.647 \times 10^5$	$4.752 \times 10^7$	11.167	16.387
	$\beta$ ( $\mu\text{g g}^{-1}$ )	0.191	0.412	0.107	0.241
	$R^2$	0.977	0.866	0.990	0.983
	$\Delta q_e$ (%)	1.523	3.145	25.866	4.545
	SSE	0.108	0.310	1.601	0.182
Intraparticle diffusion	$K_{id}$ ( $\mu\text{g g}^{-1} \text{min}^{1/2}$ )	3.204	1.390	6.037	2.670
	$C_{id}$	60.477	40.975	0.349	5.134
	$R^2$	0.873	0.620	0.972	0.969
	$\Delta q_e$ (%)	4.124	4.398	36.213	14.820
	SSE	0.823	0.824	3.835	0.808
Pseudo-first-order	$K_1$ ( $\text{h}^{-1}$ )	0.066	0.113	0.057	0.055
	$q_e$ ( $\mu\text{g g}^{-1}$ )	16.824	6.187	34.988	15.470
	$R^2$	0.939	0.879	0.981	0.986
	$\Delta q_e$ (%)	2.017	2.083	15.163	15.203
	SSE	0.697	0.644	4.774	1.000
Pseudo-second-order	$K_2$ ( $\text{g } \mu\text{g}^{-1} \text{h}^{-1}$ )	0.038	0.075	0.001	0.021
	$q_e$ ( $\mu\text{g g}^{-1}$ )	77.519	48.780	60.606	19.763
	$R^2$	0.976	0.994	0.988	0.987
	$\Delta q_e$ (%)	2.183	0.767	15.316	7.596
	SSE	0.179	0.012	3.395	0.497
<i>Isotherm parameters</i>					
Freundlich	$K_f$ ( $\mu\text{g}^{1-(1/n)} \text{mL}^{-1/n} \text{g}^{-1}$ )	2.417	0.030	4.099	4.837
	$1/n$	1.539	2.533	1.020	1.001
	$R^2$	0.927	0.931	1.000	1.000
	$\Delta q_e$ (%)	21.442	33.264	2.951	3.202
	SSE	6.893	9.222	0.117	0.036
Langmuir	$b$ ( $\text{mL } \mu\text{g}^{-1}$ )	-0.053	-0.037	-0.004	-0.011
	$q_m$ ( $\mu\text{g g}^{-1}$ )	-69.930	-16.694	-909.091	-416.667
	$R^2$	0.876	0.838	0.998	1.000
	$\Delta q_e$ (%)	26.456	37.102	3.177	6.992
	SSE	8.729	17.391	0.101	1.892
Elovich	$K_E$ ( $\text{mL } \mu\text{g}^{-1}$ )	-0.027	-0.014	-0.006	0.002
	$q_m$ ( $\mu\text{g g}^{-1}$ )	-185.185	-66.667	-666.7	2000.000
	$R^2$	0.615	0.919	0.797	0.134
	$\Delta q_e$ (%)	22.460	19.800	2.480	3.442
	SSE	13.866	9.171	0.054	0.029
Redlich-Peterson	$K_R$ ( $\text{mL g}^{-1}$ )	2.417	0.029	4.100	1.780
	$\beta$	-0.539	-1.533	-0.020	-0.001
	$R^2$	0.543	0.715	0.483	0.089
	$\Delta q_e$ (%)	24.338	42.186	3.975	70.664
	SSE	16.265	15.191	0.130	56.683

model exhibited good fit to the adsorption process of different pesticides, including fenitrothion, trifluralin, 2,4-D, carbofuran, glyphosate, and diuron (Carneiro et al. 2015;

Lule and Atalay 2014; Pandiarajan et al. 2018). However, it was found that the pseudo-first-order kinetic equation was the most appropriate model for adsorption of 2,4-D,





methyl parathion, atrazine, and DDT (Ahmed et al. 2018; Gupta et al. 2011).

### Adsorption and desorption isotherm of thiobencarb in soil

In clay soil and sandy clay loam soil, the adsorption–desorption isotherm of thiobencarb was investigated at initial concentrations ranging from 10 to 50  $\mu\text{g}/\text{mL}$  (Fig. 3). In both soil types, adsorption occurred in a similar pattern, with statistical differences at all initial concentrations, where clay soil exhibited higher adsorption than other soil type. At initial thiobencarb concentrations of 10, 20, 30, 40, and 50  $\mu\text{g}/\text{mL}$ , thiobencarb adsorbed to clay soil is calculated to be 20.90, 56.18, 82.85, 126.43, and 147.02  $\mu\text{g}/\text{g}$ , and to sandy clay loam soil is calculated to be 7.49, 20.67, 55.95, 79.69, and 121.75  $\mu\text{g}/\text{g}$ , respectively. It is apparent that the quantity of thiobencarb adsorbed on clay soil and sandy clay loam soil correlates positively with the initial herbicide concentration. There was a maximum equilibrium concentration of 16.45  $\mu\text{g}/\text{mL}$  in clay soil and 24.26  $\mu\text{g}/\text{mL}$  in sandy clay loam soil. Thiobencarb behavior may be affected by the slurry upon which it adsorbs (Aryal et al. 2020; Phong et al. 2008).

As thiobencarb desorption isotherms differed from its adsorption isotherms, it indicated a very large hysteresis, independent of the initial herbicide concentration. Interestingly, this result is consistent with those obtained by Mahmoudi et al. (2013) who indicated that strong hysteresis can be attributed to differences in desorption and adsorption isotherms. While hysteresis may occur during physical adsorption, their causes are unknown.

It is shown in Table 5 that the average of the adsorbed quantities for thiobencarb in clay soil was 86.68  $\mu\text{g}/\text{g}$  (55.05%, as initial concentration 100%) and in sandy clay loam soil was 57.11  $\mu\text{g}/\text{g}$  (32.30%). It is interesting to observe that the averages of the adsorption,  $K_d$ ,  $\log K_{om}$ ,  $\log K_{oc}$  and  $\log K_{clay}$  were more in clay soil compared to sandy clay loam soil. This suggests that the thiobencarb adsorption in clay soil was the highest. Based on the desorption process, the pesticide desorption rate can be

categorized into three kinds: rapid desorption, rate-limited desorption, and un-desorbed fractions (Sharer et al. 2003). Compared with sorption, desorption is significantly hampered or delayed (Sarkar et al. 2020). Therefore, the average of thiobencarb desorbed was 33.55  $\mu\text{g}/\text{g}$  soil corresponding to 33.52% from clay soil whereas, it was 28.67  $\mu\text{g}/\text{g}$  soil corresponding to 43.24% from sandy clay loam soil, based on the adsorbed quantity for each initial concentration of 100%. Clearly, thiobencarb desorbed from clay soil is less than that from sandy clay loam soil, the low release of this herbicide is a result of its strong binding with soil particles and hydrophobic properties.

### Modeling of thiobencarb adsorption–desorption isotherms

Modeling of experimental adsorption data is an essential technique in order to predict the mechanisms of different adsorption systems. By modeling the experimental values of  $q_e$  (the amount of solute adsorbed) and  $C_e$  (the equilibrium concentration) with linearized models, the equation parameters are determined, and then the isotherms are reconstructed with those parameters. Several authors have studied the modeling of pesticide adsorption–desorption isotherms (Matias et al. 2019; Narayanan et al. 2017; Pandiarajan et al. 2018; Ulfa and Iswanti 2020). The adsorption isotherm models, and their empirical and linear forms are presented in Table 2. Among other isotherm models, the Freundlich model produced the highest  $R^2$  value and lowest values of  $\Delta q_e\%$  and SSE in clay soil and sandy clay loam soil. This model can be used in adsorption processes on heterogenous solid surfaces (Ayawei et al. 2015). Although the Langmuir model showed high  $R^2$  values from 0.9 to 1.0, it also showed high  $\Delta q_e\%$  and SSE values, indicating that it is limited to explaining the experimental data of thiobencarb (Table 4). This result is consistent with those reported by (Shanavas et al. 2011), who stated that the Langmuir isotherm has only limited applicability. Moreover, the Elovich and Redlich–Peterson models give lower  $R^2$  values and higher  $\Delta q_e\%$  and SSE values compared to those produced by other isotherm models (Table 4). Therefore, both isotherm models Elovich and Redlich–Peterson are unable to describe the experimental adsorption and desorption data of thiobencarb in clay soil and sandy clay loam soil. In the literature, it has been shown that the Freundlich isotherm model was appropriate for describing experimental data for various compounds; including fenitrothion (Sakellarides and Albanis 2000), aldicarb (El-Aswad et al. 2002), spinosad (Hedia and El-Aswad 2016), 2,4-D (Matias et al. 2019; Pandiarajan et al. 2018), and metribuzin (Fouad et al. 2019).

The Freundlich parameters  $K_f$  ( $\mu\text{g}/\text{g}$ ), a coefficient indicating the sorption capacity, and  $1/n$ , a constant indicating the adsorption affinity, can be calculated from the intercept and

**Table 5** Average of adsorption and partition parameters for adsorption of thiobencarb in clay and sandy clay loam soil

Parameters	Clay soil	Sandy clay loam soil
Adsorption ( $\mu\text{g g}^{-1}$ )	86.676	57.111
$K_d$ ( $\mu\text{g g}^{-1}$ )	8.249	2.729
$\log K_{om}$	2.378	2.168
$\log K_{oc}$	2.614	2.405
$\log K_{clay}$	1.274	1.055



slope of the linearized plot  $\log q_e$  vs.  $\log C_e$ , respectively (Table 4). In clay soil and sandy clay loam soil,  $K_f$  values were 2.42 and 0.03, and  $1/n$  values were 1.54 and 2.53, respectively. A higher  $K_f$  value was observed for thiobencarb isotherm in clay soil than in sandy clay loam soil, indicating clay soil had the highest sorption capacity (Narayanan et al. 2017). A high OM content in clay soil was observed to be associated with greater thiobencarb adsorption (larger  $K_f$  value). This result is in agreement with those reported by García-Delgado et al. (2020) and El-Aswad et al. (2002), which claimed that clay loam soil shows greater ability to adsorb pesticides than sandy loam soil. Since the sandy loam soil contains a high level of calcium carbonate which reduces its ability to adsorb pesticides, that contains a high level of calcium carbonate, which may reduce its ability to adsorb pesticides. In clay soil and sandy clay loam soil,  $1/n$  values were greater than unity, indicating a low affinity between adsorbent and adsorbate at low concentrations (showing S-type isotherm) (Hedia and El-Aswad 2016). Literature also indicates that S-type isotherms are associated with clays and low organic matter soils (Kumari et al. 2020; Sakellarides and Albanis 2000). In the desorption isotherm, values of  $1/n$  for the two tested soils were unity, indicating C-type isotherm. Further, using  $1/n$  values according to (Barriuso et al. 1994), the hysteresis coefficient ( $H$ ) can be estimated using  $H = (1/n_{des}) / (1/n_{ads})$ , indicating that thiobencarb adsorption in clay soil and sandy clay loam soil is an irreversible process ( $H_{index} < 1$ ).

### Mobility of thiobencarb in soil

The results showed that the water tracer  $I^-$  leached rapidly in soil columns, the iodide applied was leached in about 1.7 L, and the highest concentrations were detected in the first 0.8 L of leachates from clay soil columns, and in the first 0.5 L of leachates from sandy clay loam soil columns (Fig. 4). Thiobencarb breakthrough curves (BTCs) in clay soil and sandy clay loam soil obtained in Fig. (4) were almost identical in shape and tended to percolate

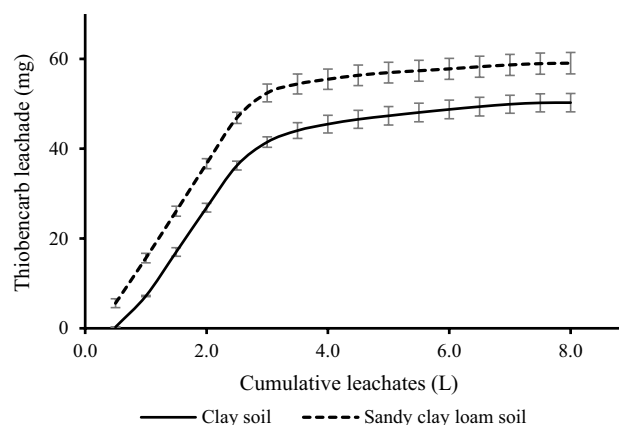


**Fig. 5** Cumulative leachate curve of thiobencarb in clay and sandy clay loam soil

within 4 L, although clay soil had longer tail. In columns of clay soil and sandy clay loam soil, respectively, the top of BTCs was flat within percolation of (1.1–2.3 L) and (0.7–2.4 L); the thiobencarb concentration in the leachates reached a maximum at the top of the peaks corresponding to about 2 L percolate. It was shown that BTCs for mobile chemicals had flatter peaks or longer tailing (Frank et al. 2021; Paswan and Sharma 2023). Based on Fig. 5, it can be seen that thiobencarb leaches significantly more readily in sandy clay loam soil than in clay soil. This result might be explained by the fact that sandy clay loam soil contains more sand and more macropores than clay soil (Hellner et al. 2018; Shipitalo et al. 1990).

In sandy clay loam soil and clay soil, the cumulative curves for thiobencarb reached a plateau at about 60 and 50 mg/leachate, respectively. According to the chemical collected in leachates and applied amounts on the column, the cumulative percentage of iodide ion recovered from the leaching process was close to 100%, and thiobencarb collected in 8 L was 67% and 79% from clay soil and sandy clay loam soil, respectively. Physicochemical properties of chemicals and soil structure determine

**Fig. 4** Breakthrough curves of thiobencarb and water tracer iodide in columns of clay soil and sandy clay loam soil. ● thiobencarb, Δ iodide

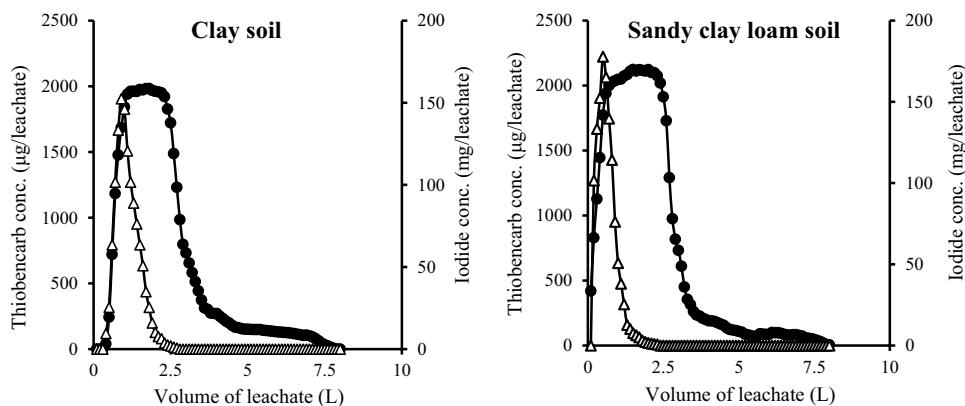


**Table 6** Prediction indicators for leaching of thiobencarb in soil

Parameters	Clay soil	Sandy clay loam soil
GUS <sub>index</sub>	1.402	1.530
RLP <sub>index</sub>	404.81	298.54

the leachability of chemicals (Shipitalo et al. 1990). The results of this experiment are in agreement with earlier results on adsorption–desorption of this compound. There is a correlation between pesticide adsorption and mobility (Aryal et al. 2020). In soil, pesticide mobility is dependent on the kinetics and mechanisms of the adsorption–desorption processes (Cueff et al. 2020). Leaching of pesticides through soil can be controlled by several factors such as flow of water and pesticide aging (Barba et al. 2020).

### Modeling of thiobencarb mobility

In many countries, mathematical mobility models have become important in the registration of pesticides (Carpio et al. 2020). There are different leaching indicators that could be used to predict pesticide leaching potentials (Arias-Estévez et al. 2008). A number of pesticides ranked by Gustafson (Bottoni et al. 1996) have a relatively high leaching potential ( $GUS > 2.8$ ), a marginal leaching potential ( $1.8 < GUS < 2.8$ ) and a low leaching potential ( $GUS < 1.8$ ). In addition, the RLP<sub>index</sub> measures leaching potential, so a lower index indicates more leaching. Data in Table 6 showed that the values of GUS<sub>index</sub> were lower than 1.8 and the RLP<sub>index</sub> values calculated were moderate for thiobencarb in tested soils. Consequently, it can be said that the leaching of herbicide thiobencarb in clay soil and sandy clay loam soil is moderate. However, the irrigation must be managed carefully to avoid excess leaching, thus protecting the groundwater resources. As well as to prevent the compound from transferring far away from the plow layer, therefore maintaining the herbicide efficiency. The leaching of pesticides depends mainly on the type of soil, agricultural practices, and pesticide properties (Cueff et al. 2020). Pesticide leaching and persistence in groundwater are important environmental aspects of pesticide application (Pérez-Lucas, 2019; Tudi et al. 2021). Herbicide activity is negatively affected by leaching in general, during heavy rain or when large amounts of irrigation water are applied, the herbicide disappears from the upper soil layers, where most weed seeds reside. Therefore, herbicides must be chosen based on their sorption and leaching characteristics in soil. Consequently, leaching results provide important

information for understanding and predicting the behavior of pesticides in soil.

### Conclusion

Thiobencarb disappeared rapidly, following the 1st-order kinetic model, where the DT<sub>50</sub> value was 10.61 days and 10.24 days for clay soil and sandy clay loam soil, respectively. Adsorption–desorption kinetics exhibited two distinct stages, early stage as a rapid and later stage as a slow. The Pseudo-second-order followed by Pseudo-first-order kinetic models and the Freundlich followed by Langmuir isotherm models fit the data for adsorption and desorption in clay and sandy clay loam soil. Compared with sandy clay loam soil, clay soil had a higher thiobencarb adsorption isotherm; however, clay soil had a lower desorption isotherm. It was observed that adsorption and mobility of thiobencarb are correlated with each other. As predicted by the leaching prediction indicators, GUS<sub>index</sub> and RLP<sub>index</sub>, thiobencarb leaches in soils (clay and sandy clay loam) at a moderate rate; however, it is highly leachable in sandy clay loam soil compared to clay soil. Practically, it is very important to take good care of irrigation, especially of rice crop. The persistence, adsorption–desorption, and leaching of thiobencarb affect the extent of the threat to groundwater resources as well as the efficacy of weed control. Furthermore, the modeling of pesticide behavior in soil reduces the cost and time compared to the experimental studies that are expensive and time consuming. Also, by modeling, the behavior of pesticides might be predicted under various conditions. Therefore, the suitable mathematical models must be used to predict the behavior of pesticides under Egyptian conditions for pest control and environmental protection as well as risk assessment. Finally, new pesticides and alternative pesticides will need to be studied and further researched in order to understand their fate and behavior.

**Author contributions** The study conception and design were proposed by MIA and AFEA. Material preparation was performed by AFEA and MRF, and analysis was performed by AFEA and MRF. The first draft of the manuscript was written by AFEA and all authors commented on previous versions of the manuscript. All authors modified and approved the final manuscript.

**Funding** Open access funding provided by The Science, Technology & Innovation Funding Authority (STDF) in cooperation with The Egyptian Knowledge Bank (EKB). The authors declare that no funds, grants, or other support were received during the preparation of this manuscript.

**Data availability** Not applicable for that section.

**Code availability** Not applicable for that section.

## Declarations

**Conflicts of interest** The authors have no relevant financial or non-financial interests to disclose.

**Consent to participate** Not applicable' for that section.

**Consent for publication** Not applicable' for that section.

**Ethics approval** Not applicable' for that section.

**Open Access** This article is licensed under a Creative Commons Attribution 4.0 International License, which permits use, sharing, adaptation, distribution and reproduction in any medium or format, as long as you give appropriate credit to the original author(s) and the source, provide a link to the Creative Commons licence, and indicate if changes were made. The images or other third party material in this article are included in the article's Creative Commons licence, unless indicated otherwise in a credit line to the material. If material is not included in the article's Creative Commons licence and your intended use is not permitted by statutory regulation or exceeds the permitted use, you will need to obtain permission directly from the copyright holder. To view a copy of this licence, visit <http://creativecommons.org/licenses/by/4.0/>.

## References

- Abdo A, Ackermann M, Ajello M et al (2010) Gamma-ray light curves and variability of bright Fermi-detected blazars. *Astrophys J* 722(1):520
- Adhya T, Wahid P, Sethunathan N (1987) Persistence and biodegradation of selected organophosphorus insecticides in flooded versus non-flooded soils. *Biol Fertil Soils* 5(1):36–40
- Ahmed SM, Taha MR, Taha OME (2018) Kinetics and isotherms of dichlorodiphenyltrichloroethane (DDT) adsorption using soil–zeolite mixture. *Nanotechnol Environ Eng* 3(1):1–20
- Al-Ghouti MA, Da'ana DA (2020) Guidelines for the use and interpretation of adsorption isotherm models: a review. *J Hazard Mater* 393:122383
- Arias-Estévez M, López-Periago E, Martínez-Carballo E, Simal-Gándara J, Mejuto J-C, García-Río L (2008) The mobility and degradation of pesticides in soils and the pollution of groundwater resources. *Agr Ecosyst Environ* 123(4):247–260
- Aryal N, Wood J, Rijal I, Deng D, Jha MK, Ofori-Boadu A (2020) Fate of environmental pollutants: a review. *Water Environ Res* 92(10):1587–1594
- Ayawei N, Ekubo AT, Wankasi D, Dikio ED (2015) Adsorption of congo red by Ni/Al-CO<sub>3</sub>: equilibrium, thermodynamic and kinetic studies. *Orient J Chem* 31(3):1307
- Badawy M, El-Aswad AF, Aly MI, Fouad MR (2017) Effect of different soil treatments on dissipation of chlorantraniliprole and dehydrogenase activity using experimental modeling design. *Int J Adv Res Chem Sci* 4(12):7–23
- Barba V, Marín-Benito JM, Sánchez-Martín MJ, Rodríguez-Cruz MS (2020) Transport of <sup>14</sup>C-prosulfocarb through soil columns under different amendment, herbicide incubation and irrigation regimes. *Sci Total Environ* 701:134542
- Barriuso E, Laird D, Koskinen W, Dowdy R (1994) Atrazine desorption from smectites. *Soil Sci Soc Am J* 58(6):1632–1638
- Bhushan L, Pathma J (2021) IMPACT OF AGRO-CHEMICALS ON ENVIRONMENT: A GLOBAL PERSPECTIVE. *PLANT CELL BIOTECHNOLOGY AND MOLECULAR BIOLOGY*:1–14
- Bondareva L, Fedorova N (2021) Pesticides: behavior in agricultural soil and plants. *Molecules* 26(17):5370. <https://doi.org/10.3390/molecules26175370>
- Bottoni P, Keizer J, Funari E (1996) Leaching indices of some major triazine metabolites. *Chemosphere* 32(7):1401–1411
- Camara MA, Fuster A, Oliva J (2020) Determination of pesticide residues in edible snails with QuEChERS coupled to GC-MS/MS. *Food Addit Contam Part A Chem Anal Control Expo Risk Assess* 37(11):1881–1887. <https://doi.org/10.1080/19440049.2020.1809720>
- Carneiro RT, Taketa TB, Neto RJG et al (2015) Removal of glyphosate herbicide from water using biopolymer membranes. *J Environ Manage* 151:353–360
- Carpio MJ, Rodríguez-Cruz MS, García-Delegado C, Sánchez-Martín MJ, Marín-Benito JM (2020) Mobility monitoring of two herbicides in amended soils: a field study for modeling applications. *J Environ Manage* 260:110161
- Chen X, Hossain MF, Duan C, Lu J, Tsang YF, Islam MS, Zhou Y (2022) Isotherm models for adsorption of heavy metals from water—a review. *Chemosphere* 307:135545
- Copaja SV, Gatica-Jeria P (2021) Effects of clay content in soil on pesticides sorption process. *J Chil Chem Soc* 66(1):5086–5092
- Cox S, Flin R (1998) Safety culture: philosopher's stone or man of straw? *Work Stress* 12(3):189–201
- Cueff S, Alletto L, Bourdat-Deschamps M, Benoit P, Pot V (2020) Water and pesticide transfers in undisturbed soil columns sampled from a Stagnic Luvisol and a Vermic Umbrisol both cultivated under conventional and conservation agriculture. *Geoderma* 377:114590
- Das SK, Mukherjee I, Kumar A (2015) Effect of soil type and organic manure on adsorption–desorption of flubendiamide. *Environ Monit Assess* 187(7):1–11
- El-Aswad AF, Fuehr F, Burauel P, Aly MI, Bakry NM (2002) Leaching Potential of Alachlor and Picloram in disturbed and undisturbed soil columns. *J Pest Contral Environmental Sci* 10(1):99–114
- El-Aswad AF, Aly MI, Fouad MR, Badawy MEI (2019) Adsorption and thermodynamic parameters of chlorantraniliprole and dinotefuran on clay loam soil with difference in particle size and pH. *J Environ Sci Health B* 54(6):475–488. <https://doi.org/10.1080/03601234.2019.1595893>
- Et A, Shahmohammadi-Kalalagh S (2011) Isotherm and kinetic studies on adsorption of Pb, Zn and Cu by kaolinite. *Caspian J Environ Sci* 9(2):243–255
- Ezzati R (2020) Derivation of pseudo-first-order, pseudo-second-order and modified pseudo-first-order rate equations from Langmuir and Freundlich isotherms for adsorption. *Chem Eng J* 392:123705
- Fardillah F, Ruhimat A, Priatna N (2020) Self-regulated learning student through teaching materials statistik based on minitab software. In: *Journal of Physics: Conference Series*, IOP Publishing, 1477: 042065
- Foo KY, Hameed BH (2010) Insights into the modeling of adsorption isotherm systems. *Chem Eng J* 156(1):2–10
- Fouad MR, El-Aswad AF, Badawy ME, Aly MI (2019) Adsorption isotherms modeling of herbicides bispyribac-sodium and metribuzin on two common Egyptian soil types. *J Agri, Environ Vet Sci* 3(2):69–91
- Fouad MR, Abou-Elnasr H, Aly M, El-Aswad A (2021) Degradation kinetics and half-lives of fenitrothion and thiobencarb in the new reclaimed calcareous soil of egypt using GC-MS. *J Adv Agri Res* 26(1):9–19
- Fouad MR (2017) Behaviour of some pesticides in soil. A Thesis Presented to the Graduate School Faculty of Agriculture, Alexandria University in Partial Fulfillment of the Requirements for the Degree of Master of Science.



- Frank S, Goepfert N, Goldscheider N (2021) Field tracer tests to evaluate transport properties of tryptophan and humic acid in karst. *Groundwater* 59(1):59–70
- García-Delgado C, Marín-Benito JM, Sánchez-Martín MJ, Rodríguez-Cruz MS (2020) Organic carbon nature determines the capacity of organic amendments to adsorb pesticides in soil. *J Hazard Mater* 390:122162
- Ge J, Cui K, Yan H et al (2017) Uptake and translocation of imidacloprid, thiamethoxam and difenoconazole in rice plants. *Environ Pollut* 226:479–485. <https://doi.org/10.1016/j.envpol.2017.04.043>
- Gupta VK, Gupta B, Rastogi A, Agarwal S, Nayak A (2011) Pesticides removal from waste water by activated carbon prepared from waste rubber tire. *Water Res* 45(13):4047–4055. <https://doi.org/10.1016/j.watres.2011.05.016>
- Gustafson DI (1989) Groundwater ubiquity score: a simple method for assessing pesticide leachability. *Environ Toxicol Chem: an Int J* 8(4):339–357
- Hamdaoui O, Naffrechoux E (2007) Modeling of adsorption isotherms of phenol and chlorophenols onto granular activated carbon. Part I. Two-parameter models and equations allowing determination of thermodynamic parameters. *J Hazard Mater* 147(1–2):381–394. <https://doi.org/10.1016/j.jhazmat.2007.01.021>
- Hedia RM, El-Aswad AF (2016) Spinosad adsorption on humic and clay constituents of lacustrine Egyptian soils and its leaching potential. *Alexandria Sci Exchange J* 37:457–466
- Hellner Q, Koestel J, Ulén B, Larsbo M (2018) Effects of tillage and liming on macropore networks derived from X-ray tomography images of a silty clay soil. *Soil Use Manag* 34(2):197–205
- Hermosín M, Cornejo J (1994) Role of soil clay fraction in pesticide adsorption. *Defining a K<sub>clay</sub>*. Royal Society of Chemistry, Environmental Behaviour of Pesticides and Regulatory Aspects London, UK
- Holliday VT (1990) Methods of soil analysis, part 1, physical and mineralogical methods, A. Klute, Ed., 1986, American Society of Agronomy, Agronomy Monographs 9 (1), Madison, Wisconsin, 1188, \$60.00. Wiley Online Library
- Hornsby JL, Mongan PF, Taylor AT, Treiber FA (1991) 'White coat' hypertension in children. *J Fam Pract* 33(6):617–624
- Itodo A, Abdulrahman F, Hassan L, Maigandi S, Itodo H (2010) Intraparticle diffusion and intraparticulate diffusivities of herbicide on derived activated carbon. *Researcher* 2(2):74–86
- Khan S, Dupont S (1987) Bound pesticide residues and their bioavailability. In: *Pesticide science and biotechnology*. In: Proceedings of the Sixth International Congress of Pesticide Chemistry held in Ottawa, Canada, 10–15 August, 1986/edited by R Greenhalgh, TR Roberts, (1987). Oxford [Oxfordshire]: Blackwell Scientific Publications
- Kumar NS, Asif M, Al-Hazzaa MI, Ibrahim AA (2018) Biosorption of 2, 4, 6-trichlorophenol from aqueous medium using agrowaste: pine (*Pinus densiflora* Sieb) bark powder. *Acta Chim Slov* 65(1):221–230
- Kumari U, Singh SB, Singh N (2020) Sorption and leaching of flucetosulfuron in soil. *J Environ Sci Health B* 55(6):550–557
- Likas DT, Tsiropoulos NG (2007) Behaviour of fenitrothion residues in leaves and soil of vineyard after treatment with microencapsulate and emulsified formulations. *Int J Environ Anal Chem* 87(13–14):927–935
- Lopez-Lopez T, Martinez-Vidal JL, Gil-Garcia MD, Martinez-Galera M, Rodriguez-Lallena JA (2004) Benzoylphenylurea residues in peppers and zucchinis grown in greenhouses: determination of decline times and pre-harvest intervals by modelling. *Pest Manag Sci* 60(2):183–190. <https://doi.org/10.1002/ps.812>
- Lule GM, Atalay MU (2014) Comparison of Fenitrothion and Trifluralin adsorption on Organo-zeolites and activated carbon Part I: pesticides adsorption isotherms on adsorbents. *Particul Sci Technol* 32(4):418–425
- Lykogianni M, Bempelou E, Karamaouna F, Aliferis KA (2021) Do pesticides promote or hinder sustainability in agriculture? The challenge of sustainable use of pesticides in modern agriculture. *Sci Total Environ* 795:148625
- Mahmoudi M, Rahnemaie R, Es-haghi A, Malakouti MJ (2013) Kinetics of degradation and adsorption–desorption isotherms of thiobencarb and oxadiargyl in calcareous paddy fields. *Chemosphere* 91(7):1009–1017
- Manohar D, Noeline B, Anirudhan T (2006) Adsorption performance of Al-pillared bentonite clay for the removal of cobalt (II) from aqueous phase. *Appl Clay Sci* 31(3–4):194–206
- Martínez-Vitela MA, Gracia-Fadrigue J (2020) The Langmuir-Gibbs surface equation of state. *Fluid Phase Equilib* 506:112372
- Matias CA, Vilela PB, Becegado VA, Paulino AT (2019) Adsorption kinetic, isotherm and thermodynamic of 2, 4-dichlorophenoxyacetic acid herbicide in novel alternative natural adsorbents. *Water Air Soil Pollut* 230(12):1–13
- Mojiri A, Zhou JL, Robinson B et al (2020) Pesticides in aquatic environments and their removal by adsorption methods. *Chemosphere* 253:126646
- Narayanan N, Gupta S, Gajbhiye VT, Manjiaiah KM (2017) Optimization of isotherm models for pesticide sorption on biopolymer-nanoclay composite by error analysis. *Chemosphere* 173:502–511. <https://doi.org/10.1016/j.chemosphere.2017.01.084>
- Nelson DW, Sommers LE (1996) Total carbon, organic carbon, and organic matter. *Methods of Soil Anal Part 3 Chem Methods* 5:961–1010
- Palma G, Demanet R, Jorquera M, Mora M, Briceño G, Violante A (2015) Effect of pH on sorption kinetic process of acidic herbicides in a volcanic soil. *J Soil Sci Plant Nutr* 15(3):549–560
- Pan B, Xing B (2010) Adsorption kinetics of 17 $\alpha$ -ethinyl estradiol and bisphenol A on carbon nanomaterials. I. Several concerns regarding pseudo-first order and pseudo-second order models. *J Soils Sediments* 10(5):838–844
- Pandiarajan A, Kamaraj R, Vasudevan S, Vasudevan S (2018) OPAC (orange peel activated carbon) derived from waste orange peel for the adsorption of chlorophenoxyacetic acid herbicides from water: adsorption isotherm, kinetic modelling and thermodynamic studies. *Bioresour Technol* 261:329–341. <https://doi.org/10.1016/j.biortech.2018.04.005>
- Paswan A, Sharma PK (2023) Two-dimensional modeling of colloid-facilitated contaminant transport in groundwater flow systems with stagnant zones. *Water Res* 59(2):2022033130
- Peek DC, Appleby AP (1989) Phytotoxicity, adsorption, and mobility of metribuzin and its ethylthio analog as influenced by soil properties. *Weed Sci* 37(3):419–423
- Pérez-Lucas G, Vela N, El Aatik A, Navarro S (2019) Environmental risk of groundwater pollution by pesticide leaching through the soil profile. *Pesticides-use and misuse and their impact in the environment*, 1–28.
- Phong TK, Watanabe H, Nishimura T, Toyoda K, Motobayashi T (2008) Behavior of simetryn and thiobencarb in rice paddy lysimeters and the effect of excess water storage depth in controlling herbicide run-off. *Weed Biol Manage* 8(4):243–249
- Rahman M, Awal MA, Misbahuddin M (2020). Pesticide application and contamination of soil and drinking water. <https://www.researchgate.net/publication/3445958274>.
- Rajahmundry GK, Garlapati C, Kumar PS, Alwi RS, Vo DVN (2021) Statistical analysis of adsorption isotherm models and its appropriate selection. *Chemosphere* 276:130176
- Redondo M, Ruiz M, Boluda R, Font G (1994) Determination of thiobencarb residues in water and soil using solid-phase extraction discs. *J Chromatogr A* 678(2):375–379
- Rodrigues AE, Silva CM (2016) What's wrong with Lagergreen pseudo first order model for adsorption kinetics? *Chem Eng J* 306:1138–1142





- Sakellarides TM, Albanis TA (2000) A new organophosphorus insecticides removal process using fly ash. *Int J Environ Anal Chem* 78(3–4):249–262
- Sarkar B, Mukhopadhyay R, Mandal A, Mandal S, Vithanage M, Biswas JK (2020) Sorption and desorption of agro-pesticides in soils. In *Agrochemicals detection, treatment and remediation*, 189–205. Butterworth-Heinemann.
- Scholz-Starke B, Egerer S, Schäffer A, Toschki A, Roßig M (2017) Higher-tier multi-species studies in soil: prospects and applications for the environmental risk assessment of pesticides. In: *Ecotoxicology and Genotoxicology*. 31–58
- Shanavas S, Kunju AS, Varghese HT, Panicker CY (2011) Comparison of Langmuir and Harkins-Jura adsorption isotherms for the determination of surface area of solids. *Oriental J Chem* 27(1):245
- Shankar A, Kongot M, Saini VK, Kumar A (2020) Removal of pentachlorophenol pesticide from aqueous solutions using modified chitosan. *Arab J Chem* 13(1):1821–1830
- Sharer M, Park JH, Voice TC, Boyd SA (2003) Aging effects on the sorption–desorption characteristics of anthropogenic organic compounds in soil. *J Environ Qual* 32(4):1385–1392
- Shipitalo M, Edwards W, Owens L, Dick W (1990) Initial storm effects on macropore transport of surface-applied chemicals in no-till soil. *Soil Sci Soc Am J* 54(6):1530–1536
- Sondhia S (2019) Environmental fate of herbicide use in Central India *Herbicide Residue Research in India*. Springer
- Spadotto CA (2002) Screening method for assessing pesticide leaching potential. *Pesticidas: Revista de Ecotoxicologia e meio Ambiente*, 12: 69–78
- Spuler MJ, Briceño G, Duprat F, Jorquera M, Céspedes C, Palma G (2019) Sorption kinetics of 2, 4-D and diuron herbicides in a urea-fertilized Andisol. *J Soil Sci Plant Nutr* 19:313–320
- Sun K, Keiluweit M, Kleber M, Pan Z, Xing B (2011) Sorption of fluorinated herbicides to plant biomass-derived biochars as a function of molecular structure. *Biores Technol* 102(21):9897–9903
- Sundaram K (1994) Adsorption behavior of RH-5992 insecticide onto sandy and clay loam forest soils. *J Environ Sci Health B* 29(3):415–442
- Tian BB, Zhou JH, Xie F, Guo QN, Zhang AP, Wang XQ, Yang H (2019) Impact of surfactant and dissolved organic matter on uptake of atrazine in maize and its mobility in soil. *J Soils Sediments* 19:599–608
- Tudi M, Daniel RH, Wang L, Lyu J, Sadler R, Connell D, Phung DT (2021) Agriculture development, pesticide application and its impact on the environment. *Int J Environ Res Public Health* 18(3):1112
- Ulfa M, Iswanti Y, Ibuprofen (2020) Adsorption Study by Langmuir, Freundlich, Temkin and Dubinin-Radushkevich Models Using Nano Zinc Oxide from Mild Hydrothermal Condition. In: *IOP Conference Series: Materials Science and Engineering*, IOP Publishing, 833: 012096
- Vareda JP (2023) On validity, physical meaning, mechanism insights and regression of adsorption kinetic models. *J Mol Liquids*. <https://doi.org/10.1016/j.molliq.2023.121416>
- Vogel AI, Mendham J, Denney R, Barnes J, Thomas M (2009) *Vogel's Quantitative Chemical Analysis*. Pearson
- Wauchope RD, Buttler TM, Hornsby AG, Augustijn-Beckers PW, Burt JP (1992) The SCS/ARS/CES pesticide properties database for environmental decision-making. *Rev Environ Contam Toxicol* 123:1–155
- Yang C (1998) Statistical mechanical study on the freundlich isotherm equation. *J Colloid Interface Sci* 208(2):379–387. <https://doi.org/10.1006/jcis.1998.5843>
- Yang Q, Lu L, Xu Q, Tang S, Yu Y (2021) Using post-graphene 2D materials to detect and remove pesticides: recent advances and future recommendations. *Bull Environ Contam Toxicol* 107(2):185–193
- Yuan S, Li C, Zhang Y et al (2020) Degradation of parathion methyl in bovine milk by high-intensity ultrasound: degradation kinetics, products and their corresponding toxicity. *Food Chem* 327:127103

